Performance Analysis of CNN and Separable CNN for Land Use and Land Cover Classification in VHR Images Using Object-Oriented Approach with eXplainable Artificial Intelligence

Yilmaz E.O.[1*] and Kavzoglu T.[2]

[1] R.A., Department of Geomatics Engineering, Gebze Technical University, Turkey

[2]Prof. Dr., Department of Geomatics Engineering, Gebze Technical University, Turkey

*eoyilmaz@gtu.edu.tr

Abstract: *Land use and land cover (LULC) maps facilitate the generation of an accurate representation of the earth's evolving natural ecosystem and the influences of human activities. Thanks to the improvements in satellite technology, the technique of imagine capture may now be conducted with a remarkable degree of accuracy and periodicity. Advanced deep learning algorithms have been developed to effectively handle and precisely analyze this data. This work aims to showcase the efficacy of the deep learning models utilizing the object-based approach with Convolutional Neural Network (CNN) and separable CNN architectures. Within the CNN architecture, every filter is applied to each input channel, facilitating the acquisition of more intricate characteristics. Additionally, it exhibits superior performance when dealing with extensive datasets and intricate jobs. The Separable CNN architecture offers advanced training and decreased memory consumption due to its reduced number of parameters and computational expenses. These models used WorldView-3 imagery to create LULC maps of Akyazı district, Turkey. In the beginning, segmentation was performed with Multiresolution segmentation for the segmentation stage. Then, spectral, texture and spatial features of each segment were calculated. A dataset containing train (70%), test (15%) and validation (15%) was created for training CNN and Separable CNN models separately. The CNN model demonstrated exceptional performance across all metrics. The Kappa accuracy of this model was 92.02% and the overall accuracy was 93.10%. In contrast, the Separable CNN model exhibited lower performance compared to the CNN model, with a Kappa accuracy of 90.68% and an overall accuracy of 91.95%. Future advancements and integration of both technologies have the potential to enhance performance and efficiency, particularly in large-scale and intricate LULC projects. This work is a significant advancement in expanding the possibilities and usefulness of both CNN and Separable CNN methods in object-oriented approach.*

Keywords: *CNN, deep learning, separable CNN, LULC, object-oriented approach*

Introduction

In line with the expansion of the global population, the surface of the earth is undergoing a growing number of changes. Over the years past, the surface of the Earth has experienced changes because of human activity (Shi et al., 2023 In effect, various changes had taken place on the soil surface Earth due to human beings' actions for a period of time that extends back over fifty years. The pattern of land use and land cover (LULC) is altered because of

the transformation of arable land into built-up land and the expansion of urbanization (Timilsina et al., 2020). Land use refers to the changes that have occurred on the surface of the earth as a result of human activities or the physical alterations that have occurred on the surface of earth containing deforestation, built-up areas, landslides, urbanization, and floods. Land cover shows differences in terms of space information about vegetation soil and water found on the earth's surface (Digra et al., 2022). Alterations in LULC are a key component of remote sensing because they allow for the extraction of useful information, the processing of images, and the classification of spectral elements that represent land cover (Turner et al., 2007; Jinghua et al., 2011; Wambugu et al., 2021).

The task that is the most challenging to do is the spatial–temporal analysis of physical measurements that were carried out in large-scale landscapes. Modelling approaches were a replacement for the physical survey, and they were able to give the framework by comprehending the spatial pattern under a variety of scenarios (Digra et al. 2022). Nevertheless, the physical examine was still utilized. This is one of the factors that leads to the poor accuracy of the model, even though the physical model is more dependent on the previous knowledge of model parameters. In the recent years, a significant amount of work has been completed to automate the LULC classification (Wang et al., 2023). Recent advances in remote sensing technology have the potential to analyse large amounts of data, classify and analyse images and make predictions about future changes.

The data sources that are most essential for accurate LULC information are remote sensing images (Talukdar et al., 2020). These images present low-cost information which is both efficient and accurate observing the surface of the Earth. The range of remote sensing satellites can include coarse spatial resolution satellites such as MODIS, AVHRR, but also medium resolution Sentinel-2, high resolution WorldView, Ikonos and QuickBird (Sam & Balasubramanian, 2023; Killeen et al., 2022; Wittke et al., 2019; Wu et al., 2023). However, when it comes to acquiring broad expanses of land using high-resolution remote sensing satellite images, it becomes somehow costly. Moreover, owing to the infrequent availability of high-resolution data, recent cloud-free imagery may not be available for an area of interest. For LULC mapping, the remote sensing community has established and applied a wide variety of classification methods, particularly pixel- and object-based image analysis (OBIA) approaches (Colkesen et al., 2023; Colkesen and Kavzoglu, 2019). These techniques range from traditional methods which based on image statistics methods to more advanced machine learning methods, including Support Vector Machine and Random

Forest. The success of OBIA in precisely addressing LULC has not mitigated its constraints posed by the various classification uncertainties associated with irregular objects created during segmentation. Moreover, OBIA accuracy depends on a variety of LULC types especially in urban environments where insufficient feature extraction may occur. Furthermore, some OBIA techniques based on machine learning classifiers using conceptual or binary classifiers do not observe deep level feature extraction (Hossain & Chen, 2019).

Deep learning models, being part of machine learning techniques, are intended to handle a variety of challenges in image processing. The embedding of these models into remote sensing increases the flexibility in object representation as well as enabling high-level feature extraction from images (Han et al., 2023). Deep learning methods have also been utilized for the purpose of applying LULC mapping across diverse landscapes. Nevertheless, it is significant to note that these deep learning based LULC classification approaches have often outperformed traditional and machine learning classification techniques where there is sufficient amount training data available (Ez-zahouani et al., 2023). One of their major advantages is their capacity to automatically learn the most helpful spectral and spatial information from the training set. This enables them to assist in distinguishing between LULC classes that are spectrally similar. To put it another way, they have the capacity to enhance the amount of information that is retrieved, which in turn can improve classification outcomes for certain LULC tasks. Convolutional neural network (CNN), as a deep learning approach, has seen widespread application in a variety of classification or segmentation applications (Li et al., 2024).

This research assessed the efficiency of two different deep learning models through LULC map generation using OBIA approach. In addition, the creation of LULC maps was assisted by a high-resolution WorldView-3 image. A performance analysis was carried out through precision, recall and F1-score calculation based on LULC class. Moreover, through the process Kappa coefficients and overall accuracy were computed. Also, Explainable Artificial Intelligence (XAI) was applied for the best deep learning model to explain the model behavior.

Study Area and Dataset

The area of the research was located in Akyazı region of Sakarya city within Marmara part of Turkey (Figure 1). In this area, agriculture is the main subsistence being dependent on

mean annual rainfall of about 800mm. The common planted crops are hazelnut, wheat, beetroot, potato and different other types of vegetables; among them maize is quite common. It also includes different LULC classifications such as highways, agriculture zones, rivers, forests, urbanized settlements and industrial zones. It covers approximately 422 km^2 of agricultural land and 402 km^2 of forested area (Colkesen et al., 2023).

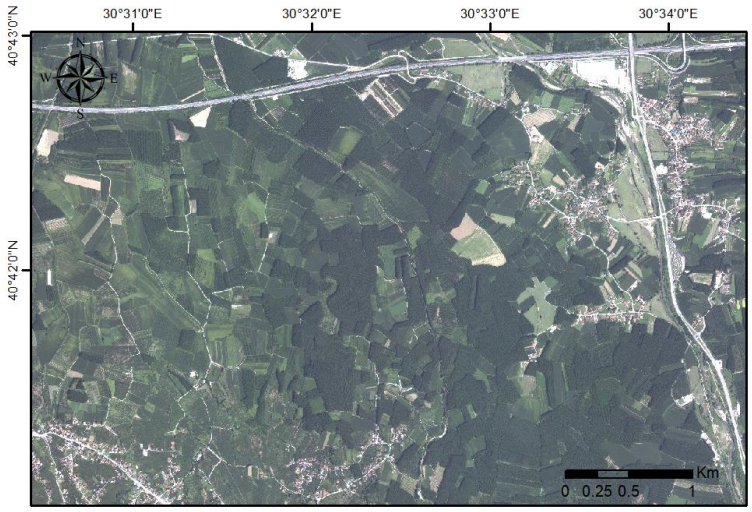

Figure 1: The study area in Sakarya-Akyazı region.

The image source was used as a WorldView-3 (WV-3) image acquired on August 15, 2021. This satellite system utilizes 8 multi-spectral bands (with a spatial resolution of 1.2 m) to obtain image. Moreover, it has an 8-band SWIR sensor which captures images with 3.7 m spatial resolution instead of 1.2 m like the other bands mentioned above Before performing LULC mapping, however, these SWIR bands were adjusted to resolve at different resolutions - namely 1.2 m using nearest neighbor method - and thereafter merged with multispectral ones according to their respective features. Moreover, LULC classes were produced by creating a thematic map of the WV-3 image. In the study area, the LULC component includes agricultural regions with their respective spaces - where multiple types formed from such activities were also found alongside poplar or hazelnut trees, bare soils, highway roads, industrial buildings, red and white roofs among other elements such as water bodies.

Methodology

Object Based Image Analysis (OBIA) is a method utilized in the assessment of remote sensing images with the objective of classifying images into meaningful objects or segments rather than

individual pixels (Kavzoglu et al., 2019; Kavzoglu & Tonbul, 2018). Segmentation is a fundamental first step in OBIA where the image is divided into smaller segments based on its spatial and spectral properties. The widely adopted multiresolution segmentation (MRS) technique is typically employed in this procedure. It treats each pixel as the smallest unit and merges these pixels with surrounding pixels that have similar characteristics to create bigger objects. The algorithm operates by using three fundamental parameters: shape, scale, and compactness (Yilmaz & Kavzoglu, 2024). The scale parameter determines the magnitude of the items, whilst the form and compactness factors govern the determination of the geometric structure of the objects. Increasing the scale parameter directly correlates with the size of the objects. Hence, selecting an appropriate scale is crucial for ensuring accurate segmentation (Tonbul & Kavzoglu, 2020). Accurate segmentation is often accomplished by a process of trial and error; however, this approach is subjective and requires a significant amount of time. Alternatively, several academics have devised ways for automatically selecting scale parameters. Local variances are calculated in the image by these means to determine the most suitable scale of segmentation. Then, during the segmentation process, objects are classified into various classes based on characteristics such as color, shape, texture etc. At this point, deep learning or machine learning algorithms are used to classify each object into its respective category. Compared to pixel-based methods OBIA provides significant advantages especially when dealing with complex terrains because it has in-built consideration for other spatial relationships during classification.

Convolutional Neural Networks (CNNs) are a crucial deep learning model employed to extract features and classify image data (Ma et al., 2019). Conventional CNNs generate feature maps by performing convolution operations on the image (Song et al., 2019). However, these operations are computationally expensive. The separable convolution approach, devised to address this issue, decreases both the computing effort and the parameter count of the model by dividing the convolution process into two separate stages (Yilmaz et al., 2022). Separable convolution involves two consecutive convolutions. The first convolution is a 1x1 convolution that extracts the spatial properties of each pixel. The following convolution establishes the link between distinct bands. This approach yields more efficient outcomes with fewer parameters in comparison to the conventional CNN and presents performance enhancements, particularly when dealing with extensive datasets. Consequently, the use of separable convolution reduces

the computational burden of CNNs, leading to the development of quicker and more lightweight models.

Explainable Artificial Intelligence (XAI) such as SHAP (Shapley Additive Explanations) methods are employed to render the decision-making processes of the model more transparent. While XAI ensures that the outputs of AI models are understandable, SHAP provides a detailed explanation of the contribution of each feature to the prediction of the model. The SHAP value enables the determination of the order of importance of the features for each example, thus facilitating a better understanding of the model's decisions. In addition to enhancing the comprehension of the model's accuracy, this approach also facilitates an understanding of the model's functioning and the factors influencing its predictions (Kavzoglu et al., 2021).

Results and Discussion

The MRS method was used in this work to generate homogeneous segments for object-oriented image classification. The ESP-2 created by Drăgut et al. (2014) was employed to determine automatically the best scale parameter for the two images. According to the ESP results, 40 was selected as the optimal scale level. For the image the shape and compactness parameters were set to 0.3 and 0.7 respectively. A total of 134,433 image segments were created based on these parameter choices. A variety of statistical and metric characteristics were computed for each individual segment after segmentation process. By means of these qualities, the aim was to search for a more complete knowledge concerning geometric and spectral aspects of every segment. This included area segments, brightness values as well as textures based on GLCM. Additionally, the highest pixel value, lowest pixel value, average pixel value, standard deviation and NDVI index were calculated per segment in different bands within frequency spectra. Also, perimeter length-width ratios of segments' shapes were determined regarding geometric features with those computations providing comprehensive analysis for each segment considering both spectral and geometric aspects.

In the classification stage, the study worked with two deep learning models which were dissimilar: SeparableConv1D and Conv1D. These models are made to perform similarly and with a similar underlying architecture. While SeparableConv1D distinguishes itself from standard Conv1D model by its separable structure. In this method, each filter is first applied independently in spatial (width) direction, then depth direction, thus reducing processing costs and number of parameters involved. When dealing with an extensive set of data, this strategy allows a more efficient outcome acquisition. Both models used Batch

Normalization and Dropout layers to enhance deep learning network performance. In addition to that, these layers allow for fast balanced model training whilst helping reduce chances of overfitting too much on the data set being modeled during neural net fitting process. Finally, at the end stages of the model, a one-dimensional format was used via the Flatten layer on the data before several Dense layers were applied for classification purposes in order to determine how effective both models were during training over a total period comprising 900 epochs. During the training stage, each update was carried out in mini batches of 32, and the Adamax optimization algorithm was utilized in order to optimize the learning process. This optimization algorithm is a derivation of the Adam algorithm, and it is prominently recognized for its capacity to learn in a consistent and efficient manner, particularly in high-dimensional areas (Vani et al., 2019). Both models utilize the SoftMax activation function on the last layer and are optimized using categorical cross-entropy loss.

The learning curves graphs show how the training and validation losses and accuracies of two different deep learning models for (a) classical CNN and (b) Separable CNN change during the learning process (Figure 2). It can be observed that the training and validation losses decrease similarly, and the accuracy metrics increase over time in both models, indicating that the models learn effectively. In particular, the validation loss decreases significantly, and the validation accuracy stabilizes, indicating that the models avoid overlearning (overfitting). There is no evidence of overlearning in the graphs, as the validation loss decreases at a similar rate with training loss and the validation accuracy stabilizes later in training. These findings suggest that both models have a general generalization capacity and learn without overfitting the training dataset.

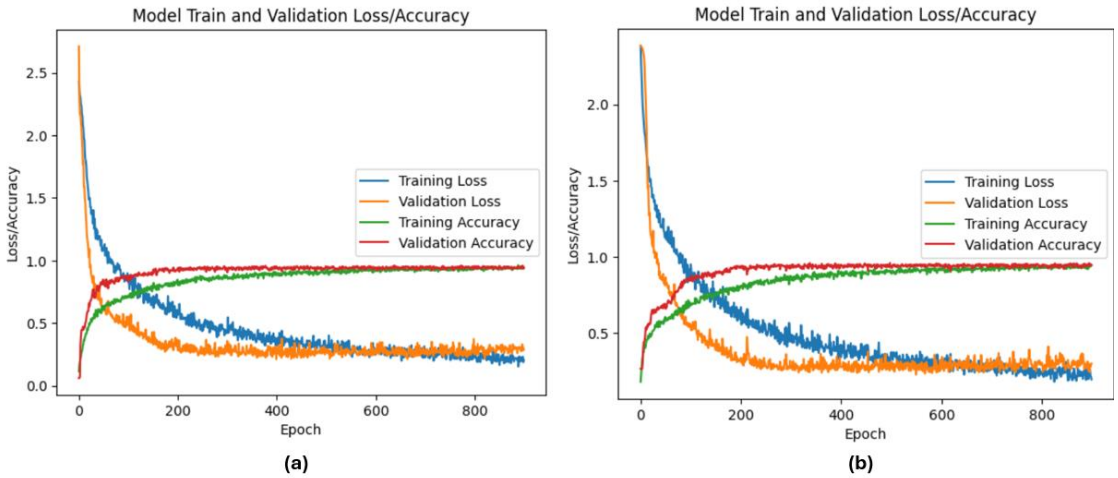

Figure 2: The learning curve of (a) CNN model and (b) Separable CNN.

This study used two distinct deep learning models, namely the conventional CNN and the Separable CNN, to assess the classification efficacy within different classes. The assessment criteria focused on accuracy, precision, recall, and F1-score (Table 1). The CNN model achieved an overall accuracy of 93.10% and a Kappa coefficient of 0.9201. In comparison, the Separable CNN model achieved an overall accuracy of 91.95% and a Kappa coefficient of 0.9069. Following executing an in-depth evaluation, it was observed that the CNN model had exceptional performance in the Hazelnut, Poplar, Young Poplar, and Water classes. The model achieved accuracy and recall rates ranging from 94% to 100% in these classes, and outstanding results were obtained for each class based on the F1-score. Specifically, the Hazelnut class scored a 100% success rate in all three metrics: accuracy, recall, and F1-score. This demonstrates that the model possesses a robust capability to precisely detect and classify these classes without any mistakes. However, although performing similarly to the standard CNN model, the Separable CNN model had lower F1-scores, particularly in the Corn, Pasture, and Red Roof classes. The F1-score shown a decline from 91% to 89% in the Corn class, from 92% to 85% in the Pasture class, and from 93% to 89% in the Red Roof class. The Separable CNN model exhibited significant reductions in accuracy and recall rates in these classes, indicating that the model has a relatively constrained ability to differentiate between these classes.

Overall, the regular CNN model exhibited superior classification performance compared to the Separable CNN model. The CNN model has superior classification capabilities, particularly in classes that demand high accuracy and recall rates. On the other hand, the Separable CNN model, while satisfactory in some classes, exhibits overall low performance. This demonstrates that, although the Separable CNN model has a less sophisticated architecture, the regular CNN model is more advantageous in deep learning methodologies, particularly for complex classes.

Figure 3 illustrates the LULC classifications generated by two distinct deep learning models. Map (a) illustrates the outcomes of the conventional CNN model, whereas map (b) depicts the findings of the Separable CNN model. Both maps depict land classes using distinct colors, effectively distinguishing several LULC types, including hazelnut, maize, grassland, poplar, and red roof. The overall geographical distributions of LULC classifications are analogous in both models. Hazelnut and poplar species were densely classified in extensive regions, but maize and grassland areas were distinctly differentiated. Both models effectively identified residential and structural elements, including red roofs,

roads, and shadows. In the Separable CNN model (b), finer features and local structures may be somewhat more pronounced; yet, for overall classification performance, both models yield comparable results. This indicates that, despite the reduced computational expense of the Separable CNN model, it yields performance results comparable to those of the traditional CNN.

Table 1: Performance Evaluation of (a) standard CNN model and (b) Separable CNN.

	CNN			Separable CNN		
Class Names	**Precision**	**Recall**	**F1-score**	**Precision**	**Recall**	**F1-score**
Hazelnut	1.00	1.00	1.00	1.00	0.97	0.98
Corn	0.93	0.90	0.91	0.90	0.88	0.89
Pasture	0.95	0.89	0.92	0.86	0.84	0.85
Poplar	0.94	1.00	0.97	0.94	1.00	0.97
Red roof	0.89	0.97	0.93	0.84	0.94	0.89
Shadow	0.98	0.95	0.96	0.98	0.96	0.97
Road	0.88	0.76	0.81	0.88	0.79	0.84
Bare soil	0.76	0.91	0.83	0.79	0.81	0.80
White roof	0.96	0.81	0.88	0.96	0.85	0.90
Water	1.00	0.86	0.92	1.0	0.86	0.92
Young poplar	1.00	0.94	0.97	1.0	0.94	0.97
Overall acc.	0.9310			0.9195		
Kappa Coef.	0.9201			0.9069		

Once the classification process was complete, SHAP analysis, one of the XAI methods, was applied to the model with the highest accuracy (Figure 4). This graph shows which features have the most influence on the model's discrimination of land cover classes. Among the features, 'Mean_Lay_4', 'Mean_Lay_3' and 'Min_pix_14' stand out as the factors that most influence the model's predictions. These features play a particularly important role in correctly identifying classes such as hazelnut (class 4), maize (class 2) and pasture (class 7). In addition, other classes, such as Blackthorn (Class 3) and Red Roof (Class 5), are also influenced by certain features that also have a significant impact on the accuracy of these classes. The SHAP plot shows that some features consistently contribute to the identification of certain classes and that these features are very important in improving the

overall performance of the model. For example, the feature ‘Mean_Lay_4’ is a particularly strong factor in discriminating between the hazelnut, maize and pasture classes. These results indicate which features the model should focus on more and provide valuable information on which features can be emphasized more to strengthen the discrimination between classes. As a result, these critical features can be used more effectively to improve the classification accuracy of the model.

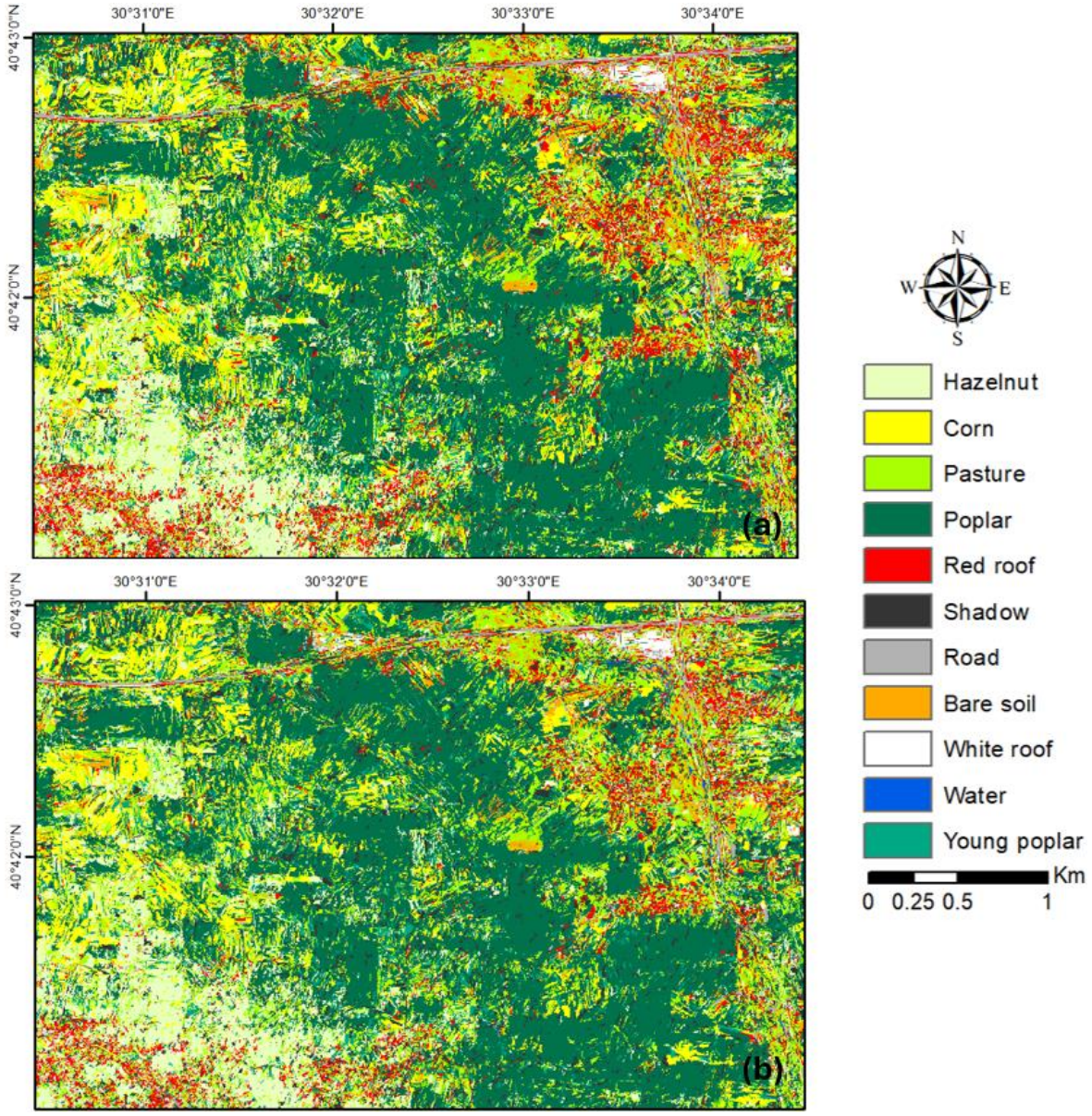

Figure 3: LULC maps produced with (a) CNN model and (b) Separable CNN model.

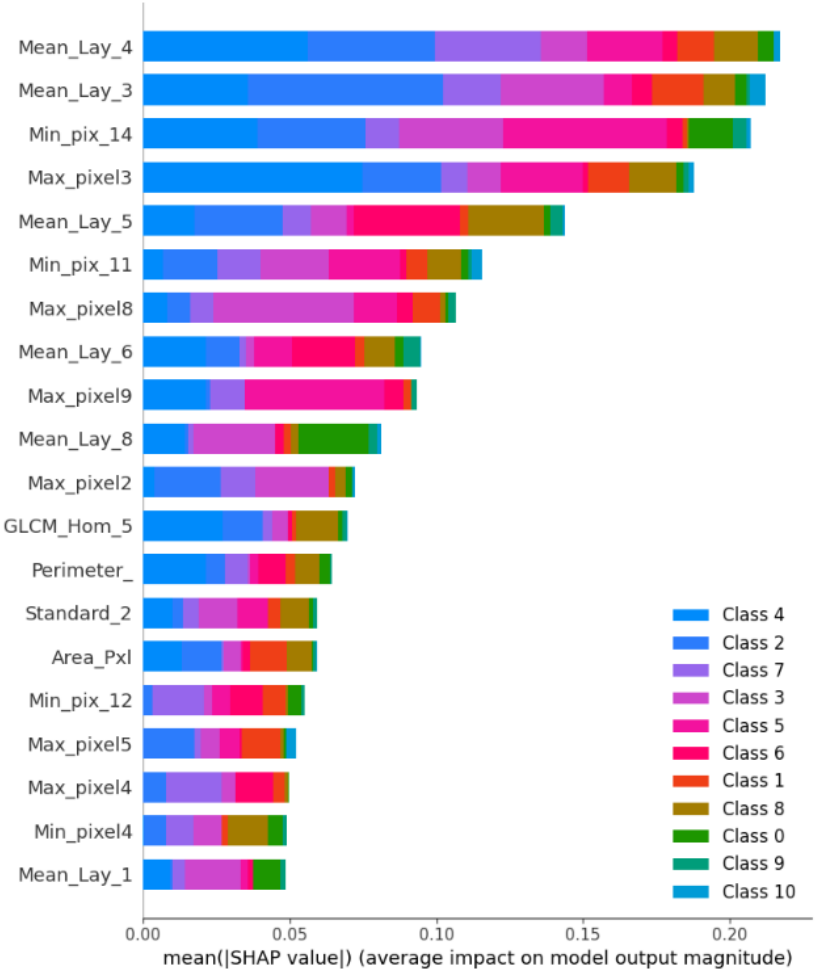

Figure 4: SHAP plot of the best performing model.

Conclusion and Recommendation

The purpose of this research is to investigate and compare the classification capabilities of CNN and Separable CNN models in the setting of the generation of a LULC thematic map. There is a significant difference between CNN and Separable CNN in terms of overall accuracy and class-based decisions, as demonstrated by the findings. The CNN model, in instance, was more effective than the Separable CNN, which had an overall accuracy of 91.95% and a Kappa coefficient of 0.9069. The CNN model had an overall accuracy of 93.10% and a Kappa value of 0.9201. It was noticed that the CNN model had a better F1-score in classes such as bare soil and road, despite the fact that both models had excellent accuracy and F1-score in classes such as Hazelnut, Young Poplar, and Water. Nevertheless, even though the Separable CNN model is more economical in terms of computation, it is not as effective as CNN since it has lower accuracy and recall values in some classes. As a result of these findings, it appears that the CNN model provides more consistent and robust

classification skills, even though the Separable CNN model offers further efficiency advantages. Moreover, according to the SHAP results of the CNN model, classes such as hazelnut, maize and pasture are more influenced by certain features and these features are key to the correct classification of these classes. SHAP analysis helps to determine which features to focus on to improve the model by showing how important certain features are in the model's decision processes. As a result, SHAP value analysis provides valuable insights to improve classification performance by showing which features are more effective in distinguishing land cover classes.

References

Colkesen, I., & Kavzoglu, T. (2019). Comparative evaluation of decision-forest algorithms in object-based land use and land cover mapping. *In Spatial Modeling in GIS and R for Earth and Environmental Sciences*, 499-517.

Colkesen, I., Kavzoglu, T., Atesoglu, A., Tonbul, H., & Ozturk, M. Y. (2023). Multi-seasonal evaluation of hybrid poplar (P. Deltoides) plantations using Worldview-3 imagery and state-of-the-art ensemble learning algorithms. *Advances in Space Research, 71(7), 3022-3044.*

Digra, M., Dhir, R., & Sharma, N. (2022). Land use land cover classification of remote sensing images based on the deep learning approaches: a statistical analysis and review. *Arabian Journal of Geosciences, 15(10), 1003*.

Drăguţ, L., Csillik, O., Eisank, C., & Tiede, D. (2014). Automated parameterisation for multi-scale image segmentation on multiple layers. *ISPRS Journal of photogrammetry and Remote Sensing, 88, 119-127.*

Ez-zahouani, B., Teodoro, A., El Kharki, O., Jianhua, L., Kotaridis, I., Yuan, X., & Ma, L. (2023). Remote sensing imagery segmentation in object-based analysis: A review of methods, optimization, and quality evaluation over the past 20 years. *Remote Sensing Applications: Society and Environment, 101031.*

Han, W., Zhang, X., Wang, Y., Wang, L., Huang, X., Li, J., ... & Wang, Y. (2023). A survey of machine learning and deep learning in remote sensing of geological environment: Challenges, advances, and opportunities. *ISPRS Journal of Photogrammetry and Remote Sensing, 202, 87-113.*

Hossain, M. D., & Chen, D. (2019). Segmentation for Object-Based Image Analysis (OBIA): A review of algorithms and challenges from remote sensing perspective. *ISPRS Journal of Photogrammetry and Remote Sensing, 150, 115-134.*

Jinghua, Z., Zhiming, F., & Luguang, J. (2011). Progress on studies of land use/land cover classification systems. *Resources Science, 33(6), 1195-1203*.

Kavzoglu, T., & Tonbul, H. (2018). An experimental comparison of multi-resolution segmentation, SLIC and K-means clustering for object-based classification of VHR imagery. *International Journal of Remote Sensing, 39(18), 6020-6036.*

Kavzoglu, T., Yilmaz, E. O., & Tonbul, H. (2019). Object-Based Land Use/Land Cover Change Detection Using Spatio-Temporal Images–A Case Study in Metropolitan City Of Istanbul, Turkey. *In The 40th Asian Conference on Remote Sensing October 2019, Daejeon, Korea.*

Kavzoglu, T., Teke, A., & Yilmaz, E. O. (2021). Shared Blocks-Based Ensemble Deep Learning For Shallow Landslide Susceptibility Mapping. Remote Sensing, 13(23), 4776.

Killeen, J., Jaupi, L., & Barrett, B. (2022). Impact assessment of humanitarian demining using object-based peri-urban land cover classification and morphological building detection from VHR Worldview imagery. *Remote Sensing Applications: Society and Environment, 27, 100766.*

Li, Z., Chen, B., Wu, S., Su, M., Chen, J. M., & Xu, B. (2024). Deep learning for urban land use category classification: A review and experimental assessment. *Remote Sensing of Environment, 311, 114290.*

Ma, L., Liu, Y., Zhang, X., Ye, Y., Yin, G., & Johnson, B. A. (2019). Deep learning in remote sensing applications: A meta-analysis and review. *ISPRS journal of photogrammetry and remote sensing, 152, 166-177.*

Sam, S. C., & Balasubramanian, G. (2023). Spatiotemporal detection of land use/land cover changes and land surface temperature using Landsat and MODIS data across the coastal Kanyakumari district, India. *Geodesy and Geodynamics, 14(2), 172-181.*

Shi, W., Zhao, X., Zhao, J., Zhao, S., Guo, Y., Liu, N., ... & Sun, M. (2023). Reliability and consistency assessment of land cover products at macro and local scales in typical cities. *International Journal of Digital Earth, 16(1), 486-508.*

Song, J., Gao, S., Zhu, Y., & Ma, C. (2019). A survey of remote sensing image classification based on CNNs. *Big Earth Data, 3(3), 232-254.*

Talukdar, S., Singha, P., Mahato, S., Pal, S., Liou, Y. A., & Rahman, A. (2020). Land-use land-cover classification by machine learning classifiers for satellite observations—A review. *Remote sensing, 12(7), 1135.*

Timilsina, S., Aryal, J., & Kirkpatrick, J. B. (2020). Mapping urban tree cover changes using object-based convolution neural network (OB-CNN). *Remote Sensing, 12(18), 3017.*

Tonbul, H., & Kavzoglu, T. (2020). Semi-automatic building extraction from Worldview-2 imagery using Taguchi optimization. *Photogrammetric Engineering & Remote Sensing, 86(9), 547-555.*

Turner, B. L., Lambin, E. F., & Reenberg, A. (2007). The emergence of land change science for global environmental change and sustainability. *Proceedings of the National Academy of Sciences, 104(52), 20666-20671.*

Vani, S., & Rao, T. M. (2019). An experimental approach towards the performance assessment of various optimizers on convolutional neural network. *In 2019 3rd international conference on trends in electronics and informatics, 11 October 2019, Tirunelveli, India.*

Wambugu, N., Chen, Y., Xiao, Z., Wei, M., Bello, S. A., Junior, J. M., & Li, J. (2021). A hybrid deep convolutional neural network for accurate land cover classification. International *Journal of Applied Earth Observation and Geoinformation, 103, 102515.*

Wang, Y., Sun, Y., Cao, X., Wang, Y., Zhang, W., & Cheng, X. (2023). A review of regional and Global scale Land Use/Land Cover (LULC) mapping products generated from satellite remote sensing. *ISPRS Journal of Photogrammetry and Remote Sensing, 206, 311-334.*

Wittke, S., Yu, X., Karjalainen, M., Hyyppä, J., & Puttonen, E. (2019). Comparison of two-dimensional multitemporal Sentinel-2 data with three-dimensional remote sensing data sources for forest inventory parameter estimation over a boreal forest. *International Journal of Applied Earth Observation and Geoinformation, 76, 167-178.*

Wu, W., Li, Z., Zhang, Z., Yan, C., Xiao, K., Wang, Y., & Xin, Q. (2023). Developing global annual land surface phenology datasets (1982–2018) from the AVHRR data using multiple phenology retrieval methods. *Ecological Indicators, 150, 110262.*

Yilmaz, E. O., & Kavzoglu, T. (2024). Quality Assessment for Multi-Resolution Segmentation and Segment-Anything Model Using WORLDVIEW-3 Imagery. *The International Archives of the Photogrammetry, Remote Sensing and Spatial Information Sciences, 48, 383-390.*

Yilmaz, E. O., Teke, A., & Kavzoglu, T. (2022). Performance evaluation of depthwise separable CNN and random forest algorithms for landslide susceptibility prediction. *In 2022 IEEE International Geoscience and Remote Sensing Symposium, 28 September 2022, Kuala Lumpur, Malaysia.*